

Treatment of Simulated Oily Wastewater by Ultrafiltration and Nanofiltration Processes

Ahmed Faiq Al-Alawy * and Mohammed Kamil Al-Ameri**

Chemical Engineering Department, College of Engineering, University of Baghdad

*Ahmedalalawy@yahoo.com, **Mohammed.k.alameri@gmail.com

Abstract

A study in the treatment and reuse of oily wastewater generated from the process of fuel oil treatment of gas turbine power plant was performed. The feasibility of using hollow fiber ultrafiltration (UF) membrane and nanofiltration (NF) membrane type polyamide thin-film composite in a pilot plant was investigated. Three different variables: pressure (0.5, 1, 1.5 and 2 bars), oil content (10, 20, 30 and 40 ppm), and temperature (15, 20, 30 and 40 °C) were employed in the UF process while TDS was kept constant at 150 ppm. Four different variables: pressure (2, 3, 4 and 5 bar), oil content (2.5, 5, 7.5 and 10 ppm), total dissolved solids (TDS) (100, 200, 300 and 400 ppm), and temperature (15, 20, 30 and 40 °C) were manipulated with the help of statistical method of Taguchi in the RO process. Analysis of variable (ANOVA) and optimum condition was investigated. The study shows that pressure has the greatest impact on the flux of UF process, while temperature and pressure have similar contribution on flux of NF process. The temperature seems to have the greatest effect on TDS rejection. It was noticed that more than 96% oil removal can be achieved with flux of 624 L/m².hr by UF process and that the fouling mechanism of UF process follows the cake/gel layer filtration model. It was observed that 100% removal of oil content can be achieved along with 79% for the TDS rejection and flux of 65 L/m².hr by NF process. The result shows fouling in NF process follows the cake filtration model. It was concluded that the observed values are within ±5% of that the predicted which reflects a strong representative model. The treated wastewater has the characteristics that it can be reused in the process to reduce the operating cost.

Key words: Taguchi, UF, NF, membrane, oily wastewater, reuse.

Introduction

A variety of industrial sources generates large amounts of wastewaters daily. Important fractions of these are the oil in water (O/W) emulsions for which current treatment technologies are often costly and ineffective [1]. Oily wastewaters are produced by various processes and

plants such as oil refineries, petrochemical plants and metalworking plants. These wastewaters create a major ecological problem throughout the world [2]. Another source of oily wastewater is the effluent of gas turbine power plants running by crude oil at which the main source of oily

wastewater is the fuel treatment process [3]. Oil in water can exist as free, dispersed, emulsified and dissolved oil. The first two forms can be separated from wastewater by simple physical processes. However, emulsified or dissolved oil is more difficult to remove [4]. Conventional oily wastewater treatment methods include gravity separation and skimming, dissolved air flotation, de-emulsification, coagulation, and flocculation. These methods have several disadvantages such as low efficiency, high operation costs, corrosion and recontamination problems [5]. With the remarkable development in membrane filtration technology these processes now exist as an efficient aid that may have all the features required by the industrial standards and environmental regulations. Hence, it is increasingly being applied for treating wastewater from different sources. Membranes have several advantages that made it applicable across a wide range of industries, such advantage like the quality of treated water (permeate) is more uniform regardless of influent variations, no chemicals are needed and the possibility for in-process recycling [6]. Membrane filtration has been proven effective in treating oily water in different industries including municipal wastewater [7], [8], engine rooms [2] and industrial wastewater [9], [10]. It was also studied in many oily wastewater treatment types of research [11], [12]. Ultrafiltration (UF) processes have been introduced as solution for oily wastewater treatment in many studies [1], [2], [9], [13], [14], however, it was noticed that UF processes fail when it comes to meet the removal of ionic contaminations, i.e., the salt ions. Reverse osmosis processes (RO) and Nanofiltration processes (NF) has found to have higher ability to remove total dissolved

solids than that of UF processes [6], [10, 11], [15-17]. Therefore, the integration of membrane processes may open the doors for efficient oily wastewater treatment and water reuse [18-20].

Taguchi Method

The conventional technique of studying the effect of multiple factors on the membrane-integrated processes may alter high cost due to a large number of runs and time besides the difficulties of interpretation of these results [21]. In such case, Taguchi approach can be applied with confined knowledge of statistics to reduce the number of runs. Hence, it was highly adopted and gained wide popularity in engineering application [22] and used in many studies related to wastewater treatment, [13], [15], [23]. Taguchi approach can be applied with confined knowledge of statistics hence, got high adaptability and gained wide popularity in engineering application [22], and used in many studies related to wastewater treatment, [13], [15], [23]. The main steps for the experimental design in Taguchi method are (1) determination the objective function, (2) identifying the control factors, (3) selection the orthogonal array (OA), (4) running the experiment, (5) analysis of the data and (6) model confirmation, [21]. Taguchi method utilizes a statistical measurement of performance known as signal-to-noise (S/N) ratio, in which signal represents the desirable value while noise represents the undesirable value. There are many different possible S/N ratios, however, two of them are applicable in the present experiments: larger is better (LTB) and small is better (STB) [22]. In this study, the larger is better (Equation 1) is the flux and TDS rejection while the smaller is better for the fouling resistant (Equation 2).

$$\left(\frac{S}{N}\right)_{LTB} = -10\log\left[\frac{1}{n}\sum_{i=1}^n \frac{1}{y_i^2}\right] \quad \dots(1)$$

$$\left(\frac{S}{N}\right)_{STB} = -10\log\left[\frac{1}{n}\sum_{i=1}^n y_i^2\right] \quad \dots(2)$$

Where S is the signal, N is the noise, n is the repetition number of each experiment with the same conditions, yi is the response of experiment.

Fouling Resistance and Filtration Model

Permeate flux and fouling resistance are key factors for UF and NF process evaluation. Flux shows the amount of permeate rate. Fouling resistance shows the significance of cake/gel layer on the membrane surface and its effect on flux decline. Fouling resistance (Rf) was calculated as following [29]:

$$R_f = \frac{TMP}{\mu} \left(\frac{1}{J_{ww}} - \frac{1}{J_{wi}}\right) \quad \dots(3)$$

Where: TMP: is the Trans membrane pressure, μ is the water viscosity, Jwi is the initial water flux, Jww is the water flux after fouling. Membrane physical structure has an important influence on flux. If the pores are larger than the size of oil droplets, these droplets may enter the pores causing irreversible fouling. When the membrane pores are smaller than the droplets in the feed, these particles/oil droplets accumulate over the membrane surface causing the formation of a cake/gel layer. During membrane filtration, the degree of fouling depends on three main factors:

1) Operation factors 2) feed properties and 3) membrane properties. the operational parameters are such an important factors in deciding the rate of membrane fouling, in particular, increasing pressure enhances formation of the cake/gel layer of higher density and finally leads to complete pore blocking [30].

Most models of membrane fouling correlate the permeate flux with time in terms of a quadratic and/or exponential relationship by assuming pore blockage, adsorption, gel-polarization, and bio-fouling [10]. The filtration models are listed in Table 1. The standard blocking mechanism occurs when the oil droplets are smaller than that of the membrane pores which leads to an internal pore blocking. The complete blocking mechanism occurs when the oil droplets size is greater than that of the membrane pores. As results, particles/oil droplets do not enter into the membrane pores and do not permeate through the membrane. The Intermediate blocking mechanism occurs when the size of oil droplets is similar to that of membrane pores leading to the Membrane pores to be blocked near their entrances on the feed side. The cake formation mechanism occurs when the size of oil droplets is much greater than the pore size; hence they are unable to enter the membrane pores. Factors affecting this type of mechanism are oil droplets deformation, cake compression, and cake/gel layer thickness.

Table 1: Equations of Filtration Models

Filtration Model	Fouling Mechanism	Ref.
$Ln(J) = Ln(J_0) - K_b t$	Complete pore blocking	[31]
$1/J^{1/2} = 1/J_0^{1/2} - K_s t$	Standard pore blocking	[32]
$1/J = 1/J_0 - K_i t$	Intermediate pore blocking	[33]
$1/J^2 = 1/J_0^2 - K_c t$	Cake filtration	[27]

Experimental Work

Wastewater Feed

Oily wastewater feed used in this experiment was prepared using untreated crude and reverse osmosis permeates water. The mixture was then agitated for one minute using 10,000 rpm homogenizer type Ultra Turrax T46/6 by Janke and Kunkel KG. An emulsifier with hypophilic-lipophilic balance (HLB) value of 7 was added as a 1% as weight percentage of the untreated crude to ensure emulsion stabilization, the emulsifier is a proper quantities mix of Tween 85 and Span 80 both by Thomas Baker, the selection of desired HLB value and the weight percentage was based on some experiments done to evaluate the emulsion stability. It was noticed that with the above-selected conditions the emulsion can still stable for more than two weeks of observation. TDS value was controlled using lab grade NaCl by Sigma-Aldrich.

Membrane System

Figure 1 shows a schematic view of the experiment setup. The system consists of one PVC type hollow fiber UF membrane with molecular weight cutoff of 50K Dalton and surface area of 2 m². The UF membrane model BN-90 and was supplied by Guangzhou Chunke Environmental Technology Co. Ltd. from China. The system consists also of polyamide thin-film composite NF membrane type NF3-2540 by Axion USA with an active area of 2.69 m². A 100 liter glass tank and NSF BRASS 140 GPH rotary vane pump by Procon USA is driven by Procon's 1/2 HP motor where used as feed tank and RO feed pump respectively. A centrifugal pump type PKm 90 by Pedrollo Co. was used as UF feed pump. Pressure gauges are installed at the module inlet and rejection stream, flow meters used to

measure permeate and rejection flow rate, throttle valve used at the rejection stream to control the pressure. Four control factors were chosen in this work: temperature, pressure, total dissolved solids, and oil concentration, while the time was kept constant at 30 minutes, the factors and their levels are shown in Table 2. The chosen of the above operation condition was based on real wastewater collected from gas turbine power plant's wastewater treatment facility where its oil contents are 39 ppm, TDS is 150 ppm. The Taguchi design of Experiment (DOE) was used and an orthogonal array of 16 runs (L₁₆) was selected as the least number of experiments can be performed to evaluate the effects of above different factors in the UF and NF process. Flux and removal efficiency were evaluated as in Equation 4 (flux calculations) and Equation 5 (removal efficiency):

$$J = \frac{Q_p}{A_m} \quad \dots(4)$$

$$\text{Removal \%} = \frac{C_i - C_p}{C_i} \times 100 \quad \dots(5)$$

Where, J = flux, (L/hr.m²), Q_p = Permeate flow rate (L/hr) and A_m = surface area of membrane (m²), C_i and C_p are initial and permeate concentration of the property respectively.

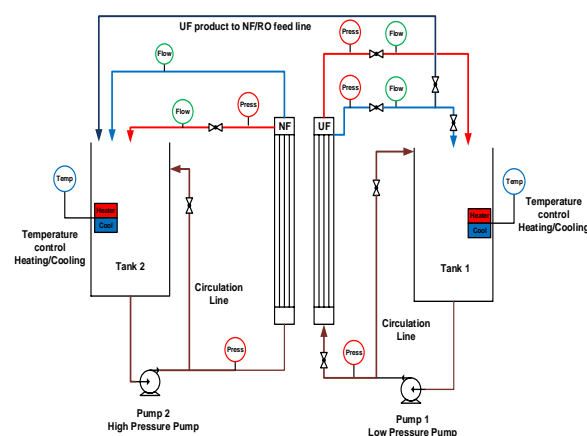


Fig. 1: Experiment Setup

Table 2: Factors Used with Their Levels

	UF Process				NF Process			
	1	2	3	4	1	2	3	4
Temp (°C)	15	20	30	40	15	20	30	40
P (bar)	0.5	1	1.5	2	2	3	4	5
TDS (ppm)	150	150	150	150	100	200	300	400
Oil (ppm)	10	20	30	40	2.5	5	7.5	10

Results and Discussion

UF Process

Table 3 represents the experimental results for UF process. It was found that oil removal for UF process exceeds the 96% for all the experimental runs, hence it was not considered as a response and was not included in the optimization process. Figure 2 represents the main effect plot for S/N ratio using the "larger is better". The figure indicates that maximizing pressure and temperature will increase the S/N ratio.

Table 3: Results of UF Process Experiments

T °C	Oil ppm	P bar	Flux LMH	Oil %	Turb.%
15	10	0.5	118.3	99.8	95.1
15	20	1.0	224.3	99.6	95.0
15	30	1.5	272.8	99.5	95.4
15	40	2.0	345.9	99.6	95.9
20	20	0.5	124.9	99.7	95.4
20	10	1.0	254.8	99.6	95.1
20	40	1.5	298.4	99.4	96.7
20	30	2.0	383.8	99.0	94.7
30	30	0.5	136.3	99.7	96.6
30	40	1.0	249.1	99.2	97.5
30	10	1.5	422.7	98.5	95.0
30	20	2.0	541.3	97.3	94.2
40	40	0.5	153.1	99.5	98.3
40	30	1.0	284.9	98.4	96.0
40	20	1.5	431.1	97.6	94.5
40	10	2.0	618.3	96.0	95.0

Figure 3 represents the effect of temperature and pressure on oil removal. It was found that higher pressure will lead to lower oil removal; this may be attributed to the fact that the increase in pressure may deform the oil droplet and push it through the pores. The temperature effect on oil

removal is increasing at elevated pressure. For example, the increase in temperature from 20 to 30 °C will decrease the oil removal by 0.2% and 2% at pressure of 0.5 and 2 bars respectively. The negative effect of temperature on the oil removal is due to the pore opening and reduction in oil viscosity.

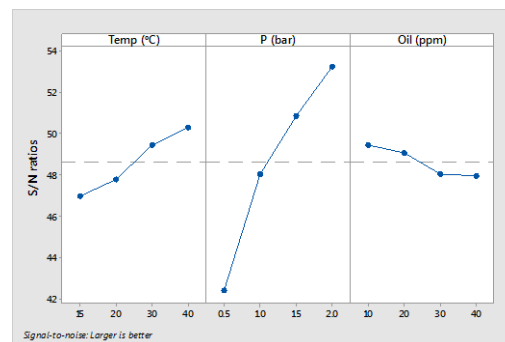


Fig. 2: S/N Ratio for Flux of UF process

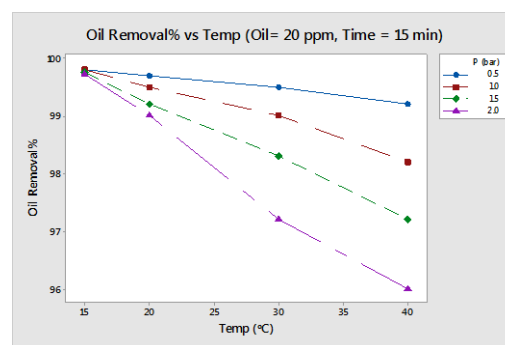


Fig. 3: Effect of Temperature and Pressure on Oil Removal

Figure 4 represents the Flux at different temperature and oil values. The figure indicates that the oil content decreases the flux linearly. The figure also indicates that the increase in oil concentration will decrease the percentage increase of flux with temperature. For example, the increase in temperature from 20 to 30 °C will

increase the flux by 7% when the oil contents are 10 ppm, however, the increase will only be 1.7% when the oil concentration is 30 ppm. This is a result of the cake layer formation which is higher when the oil concentration is high.

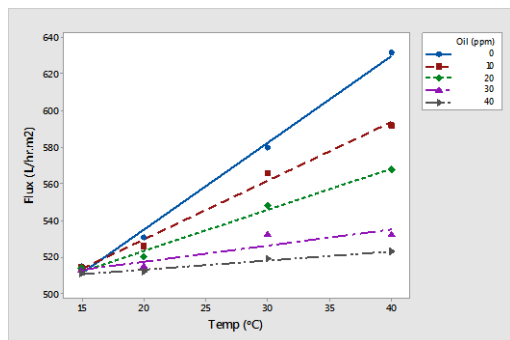


Fig. 4: Effect of Temperature on Flux of UF process at Different Oil Content (P=2 bar)

Analysis of variables was conducted for the flux data. The results are represented in Table A.1. The adequacy of the suggested model can be predicted from the residual plots of Figure 5. The ANOVA analysis suggests that the greatest contribution to the flux comes from the pressure and that P-value assumes that all the model parameters are significant. The model presented has an R^2 of 99.9%.

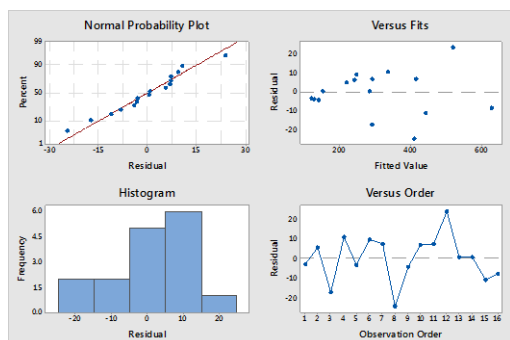


Fig. 5: Residual Plots for Flux of UF Process

The flux from experimental runs of temperature equal to 30 °C, pressure of 1 bar and oil of 20 ppm were used to evaluate the fouling mechanism. Figure 6 shows the flux decline with time. Figure 7 shows different forms of flux with time. The figure indicates

that the Cake filtration model is the best fits the experimental runs.

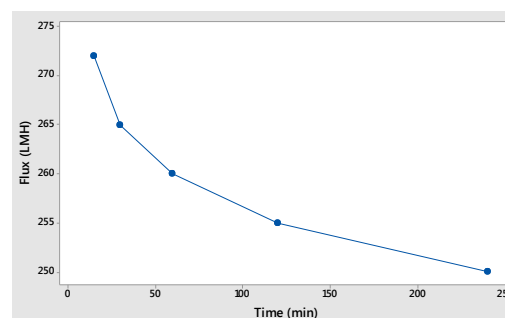


Fig. 6: Flux of UF Process vs Time

An optimization process was utilized using Minitab 17 software on UF process results. The aim of this process was to increase flux and reduce the fouling resistance. The optimum operation conditions are listed in Table 4. A confirmation experiment was conducted and the observed vs. the predicted values are shown in Table 5. The table shows that the deviation from the prediction is around 1% which reflects a strong proposed model.

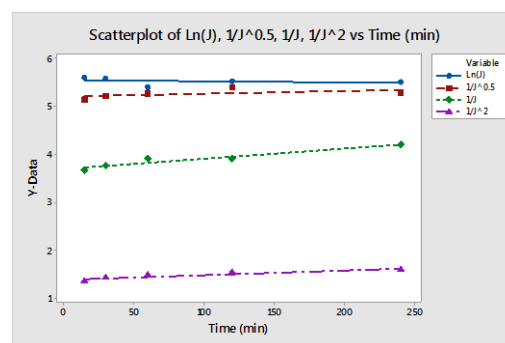


Fig. 7: Different Forms of Flux for UF Process vs. Time

Table 4: Optimum Operation Conditions for UF process

Variable	Setting
Temp (°C)	40
P (bar)	1.97
Oil (ppm)	10
Predicted Flux (L/hr.m ²)	618.3

Table 5 Predicted vs Observed Results for UF Process Confirmation Test

Parameters	Observed value	Deviation
Flux (L/hr.m ²)	624.6	1.2%
Oil Removal%	96.6	-

NF Process

Table 6 shows the L₁₆ orthogonal array results for NF process. It was found that oil removal is 100% for all the experimental runs. Hence, it will not be considered as a response and not included in the optimization process due to the high error that may be encounter in model. Figure 8 and Figure 9 represents the main effect plots for S/N of flux and TDS rejection respectively. Figure 8 show that both pressure and temperature have positive effect on flux S/N ratio increase while both oil and TDS have a negative effect. This is as the pressure increases

the driving force, temperature reduces the resistance to transfer, TDS increases the osmotic pressure and oil increases the fouling and resistance of mass transfer.

Figure 9 shows negative effect of temperature and TDS on TDS rejection S/N ratio while the effect of pressure is positive. The figures also indicate that the presence of oil in feed increases the TDS rejection and the steepest slope can be noticed at oil concentration of 7.5 to 10 ppm. This may be due to the blocking of membrane pore and reducing the salt passage.

Table 6: Experimental Results for NF process

T °C	Oil ppm	TDS ppm	P bar	Flux LMH	TDS Rejection%
15	2.5	100	2	12.2	81
15	5.0	200	3	18.6	82
15	7.5	300	4	21.0	85
15	10.0	400	5	29.5	89
20	2.5	200	4	33.2	80
20	5.0	100	5	42.5	83
20	7.5	400	2	9.5	75
20	10.0	300	3	22.0	82
30	2.5	300	5	61.0	74
30	5.0	400	4	47.1	75
30	7.5	100	3	34.0	80
30	10.0	200	2	21.0	77
40	2.5	400	3	45.5	66
40	5.0	300	2	29.7	68
40	7.5	200	5	77.0	74
40	10.0	100	4	63.5	75

The results of ANOVA for NF process are listed in Table A.2 and Table A.3 for flux and TDS rejection respectively. The analysis suggests flux modeling and TDS rejection modeling with R² of 99.67% and 99.65% respectively.

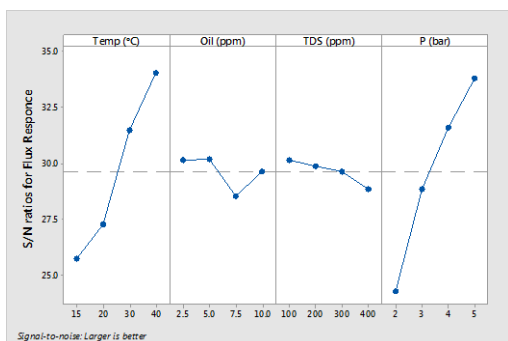


Fig. 8: S/N Ratio for Flux of NF process

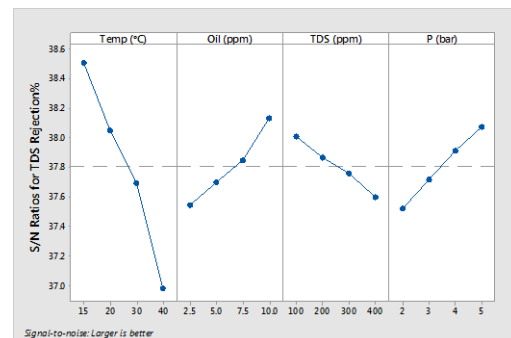


Fig. 9: S/N Ratio for TDS Rejection of NF process

Residuals versus order plot indicate that there are systematic effects in the data that may be related to the time or data collection order. Normal probability and histogram plots

showing that outlier's data do not exist. Both figures summarize that there is no obvious pattern and unusual structure. The residual analysis does not indicate model inadequacy.

Figure 12 shows the flux decline of NF process vs time at operation condition of temperature equal to 25 °C, pressure of 6 bars, oil contents of 5 ppm and TDS of 200 ppm. The flux data were represented in different forms as Ln (J), (J), 1/J0.5, 1/J and 1/J² vs time in Figure 13 which indicates that the fouling in NF process follow the cake filtration model.

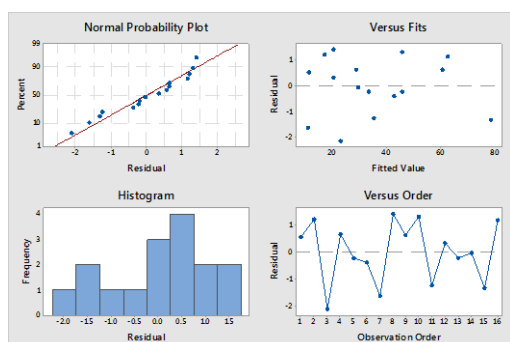


Fig. 10: Residual Plots for Flux Modeling of NF Process

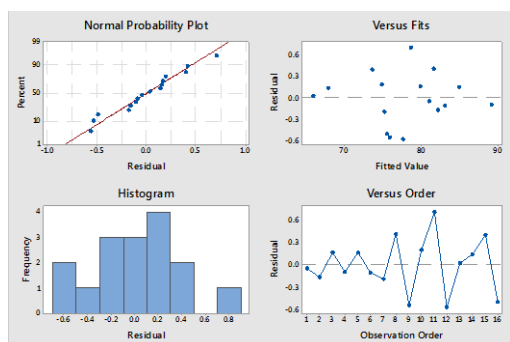


Fig. 11: Residual Plots for TDS Rejection Modeling of NF Process

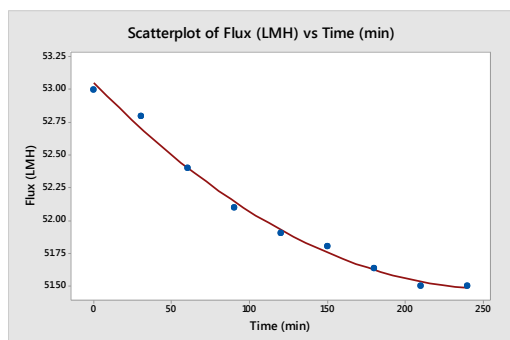


Fig. 12: Flux Decline with Time for Nf Process at Operation Condition of T= 25 C, P= 6 bar, Oil = 5 ppm And TDS =200 ppm

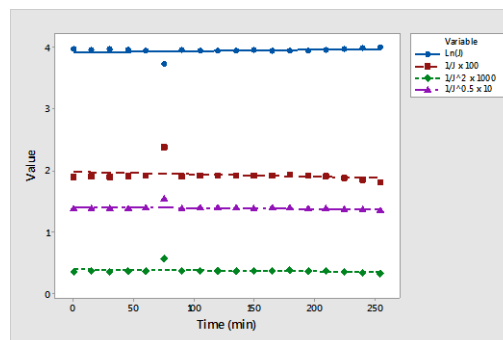


Fig. 13: Different Forms of Flux (J) With Time for NF Process at Operation Condition of T= 25 °C, P= 6 bar ,TDS= 200 ppm And Oil = 5 ppm

An optimization process was conducted using Minitab software package to increase both flux, TDS rejection and reduce the fouling resistance. The optimum operation conditions are listed in Table 7. A confirmation experiment was conducted and the observed vs. the predicted values are shown in Table 8. The table shows that the deviation from the prediction is less than 5% which reflects a strong proposed model.

Table 7: Optimum Operation Conditions for NF process

Variable	Setting
Temp (°C)	31
P (bar)	5
Oil (ppm)	7
TDS (ppm)	100
Predicted Flux (L/hr.m ²)	62.7
Predicted TDS Rej.%	78

Table 8: Predicted vs Observed Results for NF Process Confirmation Test

Parameters	Observed value	Deviation
Flux (L/hr.m ²)	65.9	4.7%
TDS Rejection%	79	1.2%
Oil Removal%	100	-

Figure 14 represents the scatter plot of the NF process flux as a response to temperature and pressure with a constant oil concentration of 5 ppm and TDS of 200 ppm. The figure shows that both temperature and pressure have a positive effect on the

flux and the effect of one parameter decreases slightly with the other parameter increase. For example, the increase of pressure from 3 to 4 bars increases the flux by 40% and 34.5% at a temperature of 20 and 40 °C respectively. Similarly, the increase in temperature from 20 to 40 °C increases the flux by 101.3% and 93% at a pressure of 3 and 4 bars respectively. These findings indicate limited effect of oil. The increase of pressure will increase the driving force, the increase in temperature increases the pore size and reduce the viscosity hence it will reduce the resistance for transfer through membrane walls.

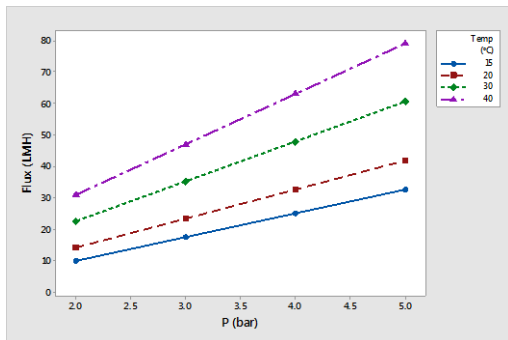


Fig. 14: Flux of NF Process vs Temperature and Pressure (TDS=200 ppm, Oil =5 ppm)

Figure 15 represents the scatter plot of the NF process flux as a response for TDS and pressure with constant temperature of 30 °c and oil concentration of 5 ppm. The figure shows a negative effect on the flux when TDS increases as a result of increasing the osmotic pressure. The effect of increasing the TDS on flux decline seems to be limited when compared with pressure. However, the decline is less at higher pressure. For example, the increase of TDS from 100 ppm to 400 ppm leads to 8.3% and 6% decrease in flux at a pressure of 3 and 4 bars respectively. Another example is that increasing the pressure from 3 to 4 bars results in 35.5% and 38.4% increase of flux at TDS equal to 100 and 400 ppm respectively.

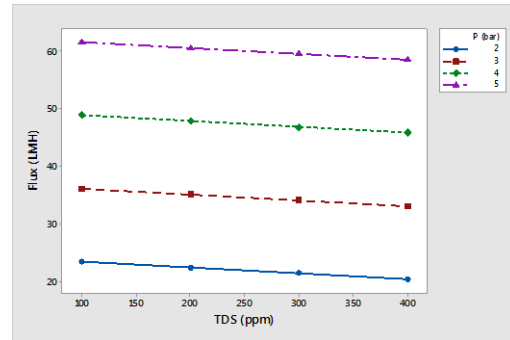


Fig. 15: Flux of NF Process vs TDS and Pressure (Temperature =30 °C, Oil =5 ppm)

Figure 16 represents the scatter plot of the flux of NF process as a response to temperature and TDS at a constant pressure of 3 bars and oil of 5 ppm. As it is the case with the TDS-Pressure effect, the TDS seems to have a lower effect on flux decline than that of temperature and this effect is decrease as the temperature increase. For example, increasing the TDS from 100 ppm to 400 ppm leads to 9% and 8.3% decrease in flux at a temperature of 20 °C and 30°C respectively. The TDS seems to have limited effect on flux increase when increasing the temperature. For example, increasing the temperature from 20 °C to 30 °C increases the flux by 48.1% and 50% at feed TDS value of 100 ppm and 400 ppm respectively.

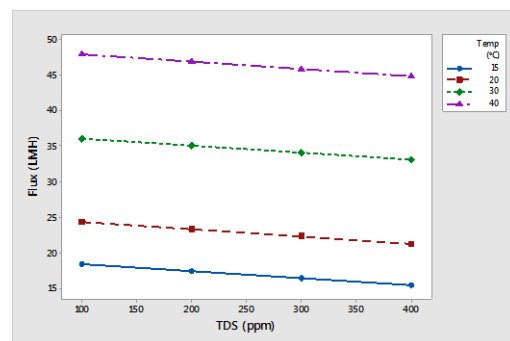


Fig. 16: Flux of NF Process vs TDS and Temperature (Pressure= 3 bars, Oil =5 ppm)

Figure 17 represents the scatter plot of the flux of NF process as a response to pressure and oil at a constant temperature of 30 °C and TDS of 200 ppm. The figure shows the negative

effect of oil on flux decline. The figure also indicates that the effect of oil is less at higher pressure. For example, the increase of oil concentration from 2.5 to 10 ppm leads to 9.1 and 4.2% decrease in pressure of 2 and 5 bars respectively.

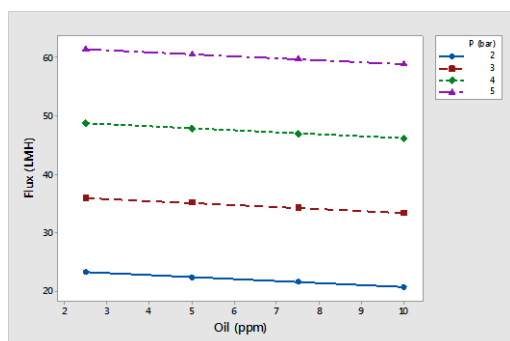


Fig. 17: Flux of NF Process vs Oil and Pressure (Temperature =30 °C, TDS =200 ppm)

Figure 18 represents the scatter plot of the flux of NF process as a response to temperature and oil at a constant pressure of 3 bars and TDS of 200 ppm. The figure shows the negative effect of oil on flux decline. The figure also indicates that the effect of oil is less at a higher temperature. For example, the increase of oil concentration from 5 to 10 ppm leads to 6.3% and 3.4% decreases in temperature of 20 and 40 °C respectively.

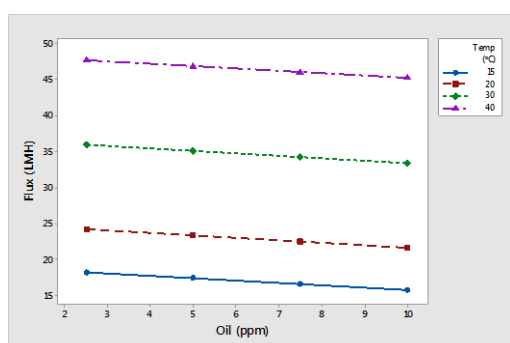


Fig. 18: Flux of NF Process vs Oil and Temperature (TDS =200 ppm, Pressure =3 bar)

Figure 19 represents the scatter plot of the flux of NF process as a response to TDS and oil at a constant pressure of 3 bars and temperature of 30 °C. The

figure shows that both oil and TDS have a negative effect on flux decline due to the increase of gel/cake layer and the concentration polarization. The increase of oil concentration from 5 to 10 ppm decreases the flux by 5%. The increase of TDS from 100 to 400 ppm decreases the flux by 8.5%.

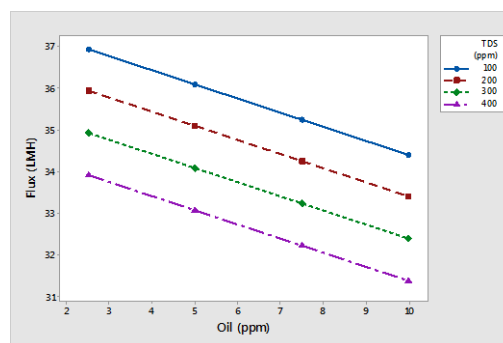


Fig. 19: Flux of NF Process vs TDS and Oil (Temperature =30 °C, Pressure =3 bar)

Figure 20 represents the scatter plot of TDS rejection percentage of NF process as a response to temperature and pressure at constant oil and TDS concentration of 5 and 200 ppm respectively. The figure shows that increasing the pressure increases the TDS rejection while increasing the temperature will decrease the TDS rejection. The figure indicates that the higher the pressure the higher effect of temperature on TDS rejection decrease and the lower the temperature the higher effect of pressure on TDS rejection increase. For example, increasing the temperature from 20 to 40 °C decreases the TDS rejection by 10.5 and 20% at pressure 3 and 4 bars respectively. Oppositely, the increase of pressure from 3 to 4 bars will increase the TDS rejection by 6 and 2.5% at a temperature of 20 and 40 °C respectively. Increasing the pressure increases the driving force of the water leading to more quantity of water to pass the membrane pore and hence more diluted permeate. The increase in temperature leads to wider membrane pore opening, an increase of solubility

of NaCl in water and decrease in water viscosity resulting in less friction with membrane walls. These can lead to salt passage and hence decrease the removal efficiency.

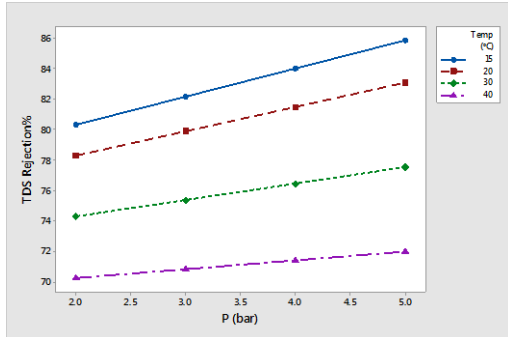


Fig. 20: TDS Rejection vs Pressure and Temperature (TDS =200 ppm, Oil =5 ppm)

Figure 21 represents the scatter plot for the TDS rejection% of NF process as a response to pressure and TDS at constant temperature value feed of 30 °C and oil of 5 ppm. The figure shows that the effect of increasing TDS is neglected at higher pressure. For example increasing TDS from 100 to 400 ppm decreases the TDS rejection by 9% at a pressure of 2 bars while it will not have any impact at a pressure of 5 bars. These findings are differing from that of oil-free feed where the TDS have a negative effect at all pressure values.

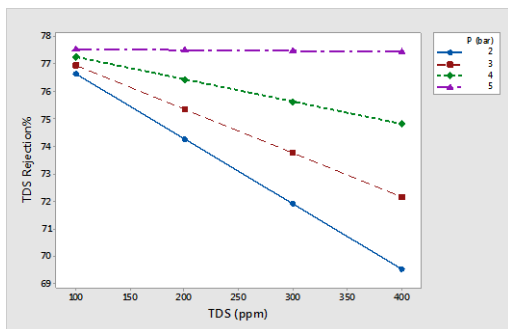


Fig. 21: TDS Rejection vs TDS and Pressure (Temperature= 30°C, Oil =5 ppm)

Figure 22 represents scatter plot for the TDS rejection% of NF process as a response to temperature and TDS at a constant pressure value of 3 bars and oil of 5 ppm. The figure shows a

negative effect of temperature and TDS concentration on the TDS rejection. It also shows that as the TDS increase, the temperature should be decreed more to maintain the TDS rejection at a specific zone.

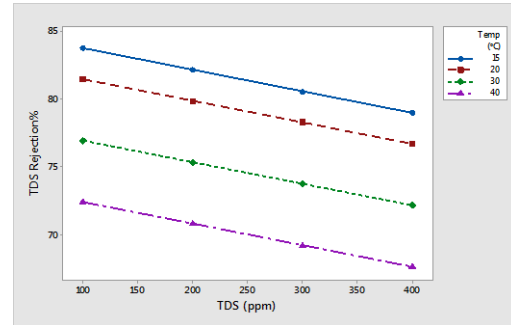


Fig. 22: TDS Rejection vs TDS and Temperature (Pressure= 3 bars, Oil =5 ppm)

Figure 23 represents scatter plot for the TDS rejection% of NF process as a response to pressure and oil at a constant temperature of 30 °C and oil concentration of 5 ppm. The figures show that increasing the oil and pressure increases the TDS rejection. This may be attributed to the fact that oil droplet will build the gel/cake layer that acts as additional resistance to the salt transfer.

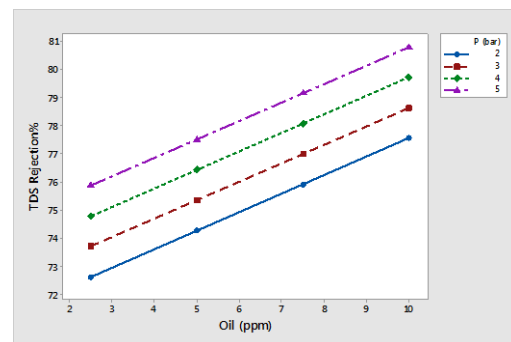


Fig. 23: TDS Rejection vs Pressure and Oil (Temperature= 30°C, TDS =5 ppm)

Figure 24 represents scatter plot for the TDS rejection% of NF process as a response to temperature and oil at a constant pressure of 3 bars and TDS concentration of 200 ppm. The figure shows that increasing the temperature decreases the TDS rejection while increasing the oil concentration will

shift the TDS rejection to a higher zone.

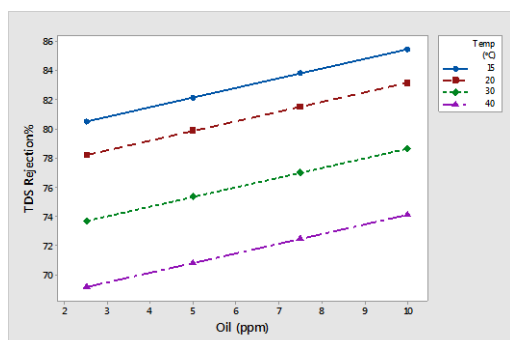


Fig. 24: TDS Rejection vs Oil and Temperature (Pressure= 3 bars, TDS =200 ppm)

Figure 25 represents scatter plot for the TDS rejection% of NF process as a response for TDS and oil at a constant pressure of 3 bars and temperature of 30 °C. The figure shows that increasing the TDS decreases the TDS rejection while increasing the oil concentration increases the TDS rejection.

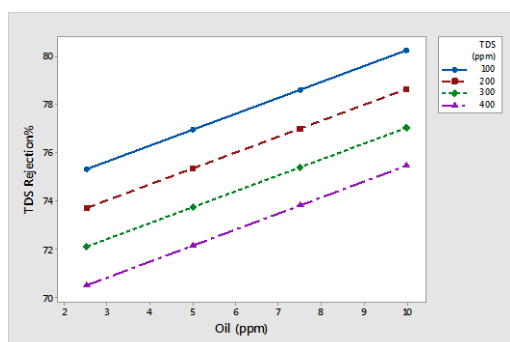


Fig. 25: TDS Rejection of NF Process vs Oil and TDS (Pressure= 3 bars, Temperature=30 °C)

Conclusions

In this study, Taguchi design of experiments (L16) was employed to analyze the different parameters contribution on the simulated oily wastewater treatment using a Hollow fibers UF membrane and polysulfone NF membrane. According to the ANOVA analysis, the most important parameter for maximum permeate flux was the pressure for UF process, while the temperature and pressure had equal effect on flux of NF process. However,

the ANOVA analysis shows that the temperature had the greatest contribution on TDS rejection. Process optimization was conducted using statistical software. Optimum conditions for UF were pressure= 2 bar, temperature= 40 °C, and oil =10 ppm. The results showed that an oil removal of 96% reached with a flux of 624.6 L/m².hr. The optimum conditions for the NF membrane to provide the highest flux and TDS rejection with the lowest resistance was found at pressure = 5 bars, TDS=100 ppm, oil =7 ppm, and temperature = 31 °C. The results showed that the treated wastewater contains no oil with low TDS value. The study suggests that the produced permeate can be reused in the process of fuel oil washing to reduce the operating cost.

Nomenclature

Symbol	Definition	Units
A_m	Membrane surface area	m ²
ANOVA	Analysis of variance	
C_f	Feed concentration	g/l
C_p	Permeate concentration	g/l
C	Concentration of solute	g/l
DOF	Degree of freedom	
HLB	Hypophilic-Lipophilic balance value	
J_{ww}	Flux after fouling	l/m ² .hr
J_{wi}	Initial Flux	l/m ² .hr
J_0	Flux of distilled water	l/m ² .hr
MS	Mean of squares	
P	Pressure	bar
μ	Viscosity	kg/(s·m)
R_f	Resistances of the foulants	1/m
SS	Sum of square	
SS_T	Total Sum of square	

<i>T</i>	Temperature	°C	<i>S/N</i>	Signal to noise
<i>TDS</i>	Total dissolved solids	ppm		ratio
<i>TMP</i>	Trans-Membrane Pressure	bar		

Appendix

Table A. 1: ANOVA of UF Experiment and Prediction Model for Flux

Source	DF	Seq SS	Contribution	Adj SS	Adj MS	F-Value	P-Value
Temp (°C)	1	17723	1.19%	849.6	849.6	48.76	0.000
P (bar)	1	1465218	98.27%	34784.8	34784.8	1996.42	0.000
Oil (ppm)	1	3839	0.26%	911.5	911.5	52.32	0.000
Temp (°C)*Temp (°C)	1	112	0.01%	111.5	111.5	6.40	0.014
P (bar)*P (bar)	1	76	0.01%	75.7	75.7	4.34	0.042
Temp (°C)*P (bar)	1	645	0.04%	644.9	644.9	37.01	0.000
Temp (°C)*Oil (ppm)	1	1774	0.12%	1774.4	1774.4	101.84	0.000
P (bar)*Oil (ppm)	1	664	0.04%	664.1	664.1	38.11	0.000
Error	55	958	0.06%	958.3	17.4		
Total	63	1491009	100.00%				

$$\text{Flux (L/m}^2\text{.hr)} = -82.71 + 3.342 \text{ Temp (}^\circ\text{C)} + 278.90 \text{ P (bar)} + 1.239 \text{ Oil (ppm)}$$

$$- 0.02033 \text{ Temp (}^\circ\text{C)}*\text{Temp (}^\circ\text{C)} - 4.35 \text{ P (bar)}*\text{P (bar)} + 0.5914 \text{ Temp (}^\circ\text{C)}*\text{P (bar)}$$

$$- 0.04905 \text{ Temp (}^\circ\text{C)}*\text{Oil (ppm)} - 0.5154 \text{ P (bar)}*\text{Oil (ppm)}$$

Table A. 2: ANOVA of NF Experiment and Prediction Model for Flux

Source	DF	Seq SS	Contribution	Adj SS	Adj MS	F-Value	P-Value
Regression	5	5606.01	99.67%	5606.01	1121.20	607.61	0.000
Temp (°C)	1	2692.58	47.87%	2.95	2.95	1.60	0.235
Oil (ppm)	1	24.31	0.43%	14.21	14.21	7.70	0.020
TDS (ppm)	1	75.86	1.35%	18.58	18.58	10.07	0.010
P (bar)	1	2616.33	46.52%	13.09	13.09	7.09	0.024
Temp (°C)*P (bar)	1	196.94	3.50%	196.94	196.94	106.73	0.000
Error	10	18.45	0.33%	18.45	1.85		
Total	15	5624.46	100.00%				

$$\text{Flux (LMH)} = -3.97 + 0.153 \text{ Temp (}^\circ\text{C)} - 0.338 \text{ Oil (ppm)} - 0.01006 \text{ TDS (ppm)} + 2.453 \text{ P (bar)} + 0.3423 \text{ Temp (}^\circ\text{C)}*\text{P (bar)}$$

Table A. 3: ANOVA of NF Experiment and Prediction Model for TDS Rejection

Source	DF	Seq SS	Contribution	Adj SS	Adj MS	F-Value	P-Value
Regression	6	534.993	99.65%	534.993	89.1656	430.51	0.000
Temp (°C)	1	381.610	71.08%	11.257	11.2572	54.35	0.000
Oil (ppm)	1	56.785	10.58%	53.870	53.8699	260.10	0.000
TDS (ppm)	1	22.684	4.23%	26.480	26.4799	127.85	0.000
P (bar)	1	55.445	10.33%	1.501	1.5014	7.25	0.025
Temp (°C)*P (bar)	1	4.391	0.82%	4.391	4.3914	21.20	0.001
TDS (ppm)*P (bar)	1	14.078	2.62%	14.078	14.0783	67.97	0.000
Error	9	1.864	0.35%	1.864	0.2071		
Total	15	536.858	100.00%				

$$\text{TDS Rejection\%} = 85.73 - 0.3006 \text{ Temp (}^\circ\text{C)} + 0.6587 \text{ Oil (ppm)} - 0.03947 \text{ TDS (ppm)} + 1.048 \text{ P (bar)} - 0.0511 \text{ Temp (}^\circ\text{C)}*\text{P (bar)} + 0.007832 \text{ TDS (ppm)}*\text{P (bar)}$$

References

1. J. Marchese, N. A. Ochoa, C. Pagliero, and C. Almandoz, "Pilot-scale ultrafiltration of an emulsified

oil wastewater," *Environ. Sci. Technol.*, vol. 34, no. 14, pp. 2990–2996, 2000.

2. K. Karakulski, A. Kozłowski, and A. W. Morawski, "Purification of oily wastewater by ultrafiltration," *Sep. Technol.*, vol. 5, no. 4, pp. 197–205, 1995.
3. H. Kaplan and K. E. Majchrzak, "Liquid Fuel Treatment Systems," GER-3481, General Electric, 1996.
4. G. R. Alther, "OILS FOUND IN WASTEWATER, What Are They?, How to Separate and Eliminate Them From Wastewater, A Layman's Guide to Emulsion Breaking," no. 248, 2014.
5. Y. S. Li, L. Yan, C. B. Xiang, and L. J. Hong, "Treatment of oily wastewater by organic-inorganic composite tubular ultrafiltration (UF) membranes," *Desalination*, vol. 196, no. 1, pp. 76–83, 2006.
6. S. Mondal and S. R. Wickramasinghe, "Produced water treatment by nanofiltration and reverse osmosis membranes," *J. Memb. Sci.*, vol. 322, no. 1, pp. 162–170, 2008.
7. K. C. Channabasappa, "Membrane technology for water reuse application," *Desalination*, vol. 23, no. 1, pp. 495–514, 1977.
8. B. Nicolaisen, "Developments in membrane technology for water treatment," *Desalination*, vol. 153, no. 1, pp. 355–360, 2003.
9. J.-J. Qin, M. H. Oo, H. Lee, and R. Kolkman, "Dead-end ultrafiltration for pretreatment of RO in reclamation of municipal wastewater effluent," *J. Memb. Sci.*, vol. 243, no. 1, pp. 107–113, 2004.
10. A. Salahi, T. Mohammadi, and F. Rekabdar, "Reverse osmosis of refinery oily wastewater effluents," *Iranian J. Environ. Health Sci. Eng.*, vol. 7, no. 5, pp. 413–422, 2010.
11. A. Orecki and M. Tomaszewska, "The oily wastewater treatment using the nanofiltration process," *Polish J. Chem. Technol.*, vol. 9, no. 4, pp. 40–42, 2007.
12. A. Rahimpour, B. Rajaeian, A. Hosienzadeh, S. S. Madaeni, and F. Ghoreishi, "Treatment of oily wastewater produced by washing of gasoline reserving tanks using self-made and commercial nanofiltration membranes," *Desalination*, vol. 265, no. 1, pp. 190–198, 2011.
13. J. K. Milić, I. Petrinić, A. Goršek, and M. Simonič, "Ultrafiltration of oil-in-water emulsion by using ceramic membrane: Taguchi experimental design approach," *Cent. Eur. J. Chem.*, vol. 12, no. 2, pp. 242–249, 2014.
14. S. Santos and M. Wiesner, "Ultrafiltration of water generated in oil and gas production," *Water Sci. Technol.*, vol. 51, no. 1, pp. 1–10, 2005.
15. S. S. Madaeni and S. Koocheki, "Application of taguchi method in the optimization of wastewater treatment using spiral-wound reverse osmosis element," *Chem. Eng. J.*, vol. 119, no. 1, pp. 37–44, 2006.
16. E. Park and S. M. Barnett, "Oil/Water Separation Using Nanofiltration Membrane Technology," *Sep. Sci. Technol.*, vol. 36, no. 7, pp. 1527–1542, 2001.
17. M. S. H. Bader, "Nanofiltration for oil-fields water injection operations: analysis of concentration polarization," *Desalination*, vol. 201, no. 1, pp. 106–113, 2006.
18. M. Tomaszewska, A. Orecki, and K. Karakulski, "Treatment of bilge water using a combination of ultrafiltration and reverse osmosis," *Desalination*, vol. 185, no. 1–3, pp. 203–212, Nov. 2005.
19. X. Yu, Z. Zhong, and W. Xing, "Treatment of vegetable oily wastewater using an integrated microfiltration-reverse osmosis system," in *Water Science and*

- Technology*, 2010, vol. 61, no. 2, pp. 455–462.
20. A. Salahi and T. Mohammadi, “Experimental investigation of oily wastewater treatment using combined membrane systems,” *Water Sci. Technol.*, vol. 62, no. 2, pp. 245–255, 2010.
 21. R. K. Roy, *A primer on the Taguchi method*. Society of Manufacturing Engineers, 2010.
 22. E. R. Ziegel, “Taguchi Techniques for Quality Engineering,” *Technometrics*, vol. 39, no. 1, pp. 109–110, 1997.
 23. A. Salahi, T. Mohammadi, R. M. Behbahani, and M. Hemmati, “Experimental investigation and modeling of industrial oily wastewater treatment using modified polyethersulfone ultrafiltration hollow fiber membranes,” *Korean J. Chem. Eng.*, pp. 1–18, 2015.
 24. N. Eliasz, G. Shemesh, and R. M. Latanision, “Hot corrosion in gas turbine components,” *Eng. Fail. Anal.*, vol. 9, no. 1, pp. 31–43, 2002.
 25. L. Yu, M. Han, and F. He, “A review of treating oily wastewater,” *Arab. J. Chem.*, 2013.
 26. I. W. Cumming, R. G. Holdich, and I. D. Smith, “The rejection of oil by microfiltration of a stabilised kerosene/water emulsion,” *J. Memb. Sci.*, vol. 169, no. 1, pp. 147–155, 2000.
 27. A. B. Koltuniewicz, R. W. Field, and T. C. Arnot, “Cross-flow and dead-end microfiltration of oily-water emulsion. Part I: Experimental study and analysis of flux decline,” *J. Memb. Sci.*, vol. 102, pp. 193–207, 1995.
 28. A. Salahi, T. Mohammadi, F. Rekabdar, and H. Mahdavi, “Reverse osmosis of refinery oily wastewater effluents,” *Iranian J. Environ. Health Sci. Eng.*, vol. 7, no. 5, p. 413, 2010.
 29. M. Kazemimoghadam and T. Mohammadi, “Chemical cleaning of ultrafiltration membranes in the milk industry,” *Desalination*, vol. 204, no. 1, pp. 213–218, 2007.
 30. S. M. Kumar and S. Roy, “Recovery of water from sewage effluents using alumina ceramic microfiltration membranes,” *Sep. Sci. Technol.*, vol. 43, no. 5, pp. 1034–1064, 2008.
 31. H. Susanto, Y. Feng, and M. Ulbricht, “Fouling behavior of aqueous solutions of polyphenolic compounds during ultrafiltration,” *J. Food Eng.*, vol. 91, no. 2, pp. 333–340, 2009.
 32. M. C. V. Vela, S. Á. Blanco, J. L. García, and E. B. Rodríguez, “Analysis of membrane pore blocking models applied to the ultrafiltration of PEG,” *Sep. Purif. Technol.*, vol. 62, no. 3, pp. 489–498, 2008.
 33. J. Kim, A. Chinen, and H. Ohya, “Membrane microfiltration of oily water,” in *Macromolecular Symposia*, 1997, vol. 118, no. 1, pp. 413–418.